

Full Film, Boundary Lubrication and Tribochemistry in Steel Circular Contacts Lubricated with Glycerol

W. Habchi · C. Matta · L. Joly-Pottuz ·
M. I. De Barros · J. M. Martin · P. Vergne

Received: 15 September 2010 / Accepted: 16 March 2011 / Published online: 1 April 2011
© Springer Science+Business Media, LLC 2011

Abstract In this article, the lubricating properties of pure glycerol are investigated under both mild and severe EHL regimes. Amazingly low friction coefficients (about 0.01) are reported by experiments in thick film regimes compared to traditional base oils. EHL calculations of film thickness and friction (including thermal effects) predict friction coefficients that are twice those actually found for glycerol. Chemical analysis of glycerol before and after the friction tests were performed by NMR and Karl Fischer methods, and they reveal that water is produced by tribochemical reaction as well as other species like aldehydes. This finding is in agreement with a corrosion pattern observed inside the wear scars of the steel samples. This study provides an explanation to the anomalously low friction observed in the thick film regime. In fact, water

produced in the lubricant decreases traction forces due to the drastic decrease of the viscosity of glycerol with water addition.

Keywords Glycerol · EHL lubrication · Tribochemistry · Water lubrication

1 Introduction, Background and Literature Survey

Under boundary lubrication regimes, ultralow friction (friction coefficients below 0.05) is very difficult to achieve with traditional additives as those used, for instance, in automotive applications. Kano et al. [1] obtained friction coefficients lower than 0.03 for contacts involving two surfaces coated with a hydrogen-free Diamond-Like Carbon coating, denoted as ta-C, and lubricated with poly-alpha olefin containing glycerol-mono-oleate (GMO). These results were explained by the formation of two OH-terminated carbon sliding surfaces and by the low energy between them. This new system was found very promising since it combines two advantages: (i) the very low friction coefficients which could contribute to a significant reduction in fuel consumption, (ii) the low toxicity of this system compared to the harmful compounds currently used in automotive lubrication. In addition, glycerol was found to exhibit very interesting lubricating properties when used to lubricate ta-C coated surfaces. Glycerol also contains alcohol chemical functionality but is a much simpler molecule than GMO. Lubrication mechanisms of both GMO and glycerol were investigated by using surface analysis (X-ray photoelectron spectroscopy ‘XPS’, Time of Flight Secondary Ion Mass Spectrometry ‘ToFSIMS’) and transmission electron microscopy [2, 3]. Computer simulations using the ReaxFF reactive force field showed that

Electronic supplementary material The online version of this article (doi:10.1007/s11249-011-9778-6) contains supplementary material, which is available to authorized users.

W. Habchi
Department of Industrial and Mechanical Engineering, Lebanese American University (LAU), Byblos, Lebanon

C. Matta (✉) · M. I. De Barros · J. M. Martin (✉)
LTDS UMR5513, Ecole Centrale de Lyon, 36 Avenue Guy de Collongue, 69134 Ecully, France
e-mail: kristine.matta@gmail.com

J. M. Martin
e-mail: jean-michel.martin@ec-lyon.fr

L. Joly-Pottuz
MATEIS UMR 5510, INSA-Lyon, Bât. Blaise Pascal, 7 Avenue Jean Capelle, 69621 Villeurbanne, France

P. Vergne
LaMCoS UMR5259, INSA-Lyon, Bât. Jean d’Alembert, 18-20 rue des Sciences, 69621 Villeurbanne, France

the sp^2 -carbon surface atoms react with glycerol and that a tribo-degradation of glycerol occurs, leading to the formation of water [4].

Glycerol has a very compact molecular structure along with specific physical properties that also confer to it a high potential as a model lubricant to study situations that still remain nowadays open questions in the lubrication field. For instance it could be used to study the Newtonian isothermal piezoviscous traction behaviour in ElastoHydrodynamic Lubrication (EHL) and to investigate the origin of the changes that occur when the operating conditions become more severe, i.e. under higher contact pressure or very thin films. Another interesting point concerns the distinction between thermal and non-Newtonian effects in EHL, both leading to similar consequences, i.e. film thickness and friction reductions. Owing to its low (92 kg/kmol) molecular weight, glycerol exhibits a high Newtonian limit and is not expected to shear-thin in the inlet region of the contact [5]. Furthermore, its very low pressure–viscosity coefficient allows quite accurate prediction of EHL friction using basic analytical models [6]. Under moderate contact pressure and entrainment speed, very low traction is achieved using this viscous fluid. On the other hand, its high viscosity and high viscosity–temperature dependence can favour inlet shear heating under appropriate conditions. This has been shown both experimentally and numerically in [7]. A fair quantitative agreement was found between experimental film thicknesses and those obtained from a full thermal EHL numerical approach.

However, until now practically no data was obtained under more severe operating conditions, for instance under high contact pressure, very thin films, high entrainment speeds or any combination of these specific cases that are representative of actual conditions encountered in mechanical systems. In this article, such severe conditions are addressed. In addition, limiting values dealing with the transition of glycerol behaviour from EHL towards the boundary regime are provided. This study also aims to propose a new contribution to the understanding of the role of water in the ultralow friction values reported under such conditions. First, a numerical study is reported to estimate film thickness and friction obtained from highly loaded steel/steel smooth EHL contacts lubricated with glycerol under a large range of entrainment speeds and slide-to-roll ratios (SRR). Then experimental results obtained under the

boundary regime (i.e. at low entrainment speed) are discussed. Karl Fischer and NMR analyses of the used glycerol samples are performed to confirm whether a chemical dissociation is taking place inside the contact or not, resulting in the generation of water. Furthermore, surface analyses are conducted to reveal any surface modifications and explore whether these could be related or not to the possible presence of water.

2 Numerical and Experimental Methods and Results

2.1 Numerical Approach

The glycerol rheological and physical properties are reported in Table 1. Rheological properties have been derived from [8, 9] whereas thermal properties can be found in [10]. Both viscosity and density of glycerol have relatively low pressure dependence. Therefore, the Cheng equation [11] appears to be appropriate to define the viscosity–pressure–temperature relationship and numerical simulations were run assuming glycerol has a Newtonian behaviour. As for the density–pressure–temperature dependence, the Tait equation of state [12, 13] is used. The solution is obtained using a fully coupled thermal EHL solver in which Reynolds, Linear Elasticity and normal load equilibrium are solved simultaneously. Then, the energy equation is solved in the solid components and the lubricant film in order to determine the temperature distribution in the contact. An iterative procedure is then established between the solutions of the EHL and Thermal EHL problems until a converged solution is attained. Finite elements are used to model both the bounding solids and the lubricating film and appropriate numerical methods are applied to obtain the solution with optimized computing time, system size and convergence rates. For more details on the thermal EHL model and the expressions used to describe the glycerol behaviour, the reader is referred to [7].

Isothermal and thermal results are reported under both pure rolling and rolling-sliding conditions for a point contact between a steel ball and a steel plane, considered as perfectly smooth. For the pure rolling case, the mean entrainment velocity covers the range from 0.005 to 5 m/s while for the rolling-sliding conditions U_e takes two

Table 1 Properties of glycerol (μ and n are measured data, α is from [8, 9] and ρ is from [10])

Temperature (K)	Viscosity μ (Pa s)	Pressure-viscosity coeff. α (GPa ⁻¹)	Density ρ (kg/m ³)	Refractive index n
313	0.293	5.4	1260	1.4661
323	0.134	5.0	1253	1.4639
353	0.0282	4.2	1234	1.4570

Table 2 Material properties and operating conditions for the TEHL simulations

Lubricant properties	Steel properties	Operating conditions
$\mu_R = 0.2803 \text{ Pa s at } T_R = 313 \text{ K}$	$\rho = 7850 \text{ kg/m}^3$	$T_0 = 323 \text{ K}$
$\alpha_{\text{Cheng}} = 5.4 \text{ GPa}^{-1}$	$k_s = 46 \text{ W/m K}$	$R = 0.0127 \text{ m}$
$\beta_{\text{Cheng}} = 7209 \text{ K}$	$c_s = 470 \text{ J/kg K}$	$w = 55 \text{ N}$
$\gamma_{\text{Cheng}} = 3900 \text{ K GPa}^{-1}$	$E_s = 210 \text{ GPa}$	$P_H = 1 \text{ GPa}$
$\rho_0 = 1253 \text{ kg/m}^3$	$\nu = 0.3$	$U_e = 0.005\text{--}5 \text{ m/s}$
$k = 0.29 \text{ W/m K}$		$\text{SRR} = 0\text{--}100\%$
$c = 2400 \text{ J/kg K}$		

constant values of 1 and 0.01 m/s with SRR varying from 0 to 100%. For all simulations, the inlet temperature is kept constant and equal to 323 K. The normal load is maintained at 55 N, leading to a Hertzian contact pressure (P_H) of 1 GPa in compliance with the objectives of this study, i.e. to study highly loaded contacts subject to more severe operating conditions compared to those previously analysed in [7]. Table 2 summarizes the material properties and operating conditions considered in the simulations.

Figure 1 shows the calculated central and minimum film thickness curves obtained under isothermal and variable temperature conditions as a function of the mean entrainment speed under pure rolling. Inlet shear heating influence is almost undetectable in Fig. 1 (partly masked by the log–log axis system). A weak deviation is nevertheless observed between isothermal and thermal results, of typically 6–11% for $U_e = 3$ and 5 m/s, respectively, regardless of the location at which film thickness is considered. Also note that at low entrainment speed, film thickness becomes extremely thin and closer to molecular size. It is important here to underline the existence of a limitation of continuum mechanics that classically considers that such an approach is no longer valid below ten molecular layers.

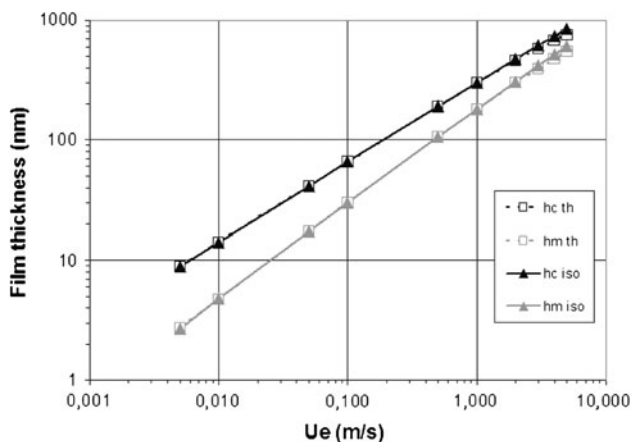


Fig. 1 Central (h_c) and minimum (h_m) film thickness versus mean entrainment velocity (U_e) predicted from isothermal and thermal EHL numerical models (glycerol, steel/steel smooth contact, pure rolling, $P_H = 1 \text{ GPa}$, $T = 323 \text{ K}$)

The slide-to-roll (SRR) influence on film thickness is shown in Table 3 for $U_e = 1 \text{ m/s}$. Film thickness variations obtained from TEHL simulations are compared to those obtained in the pure rolling case where $\text{SRR} = 0$. As for the previous film thickness results, only slight changes occur when the SRR takes significant values, revealing that inlet shear heating remains limited. Also note that simulations were run for $U_e = 0.01 \text{ m/s}$ and did not show any significant film thickness variations with SRR.

Friction coefficients are computed for both isothermal and thermal EHL regimes under the same assumptions considered before (Newtonian behaviour, smooth surfaces) for two mean entrainment velocities of 1 and 0.01 m/s. The results reported in Fig. 2 show two distinct cases: at low

Table 3 Relative film thickness variation versus SRR at $U_e = 1 \text{ m/s}$ (glycerol, steel/steel smooth contact, $P_H = 1 \text{ GPa}$, $T = 323 \text{ K}$)

SRR	$\Delta h_c/h_{c\text{SRR}=0} (\%)$	$\Delta h_m/h_{m\text{SRR}=0} (\%)$
0.20	−0.04	−0.07
0.40	−0.75	−0.76
0.60	−1.26	−1.31
0.80	−2.04	−2.04
1.00	−3.19	−3.04

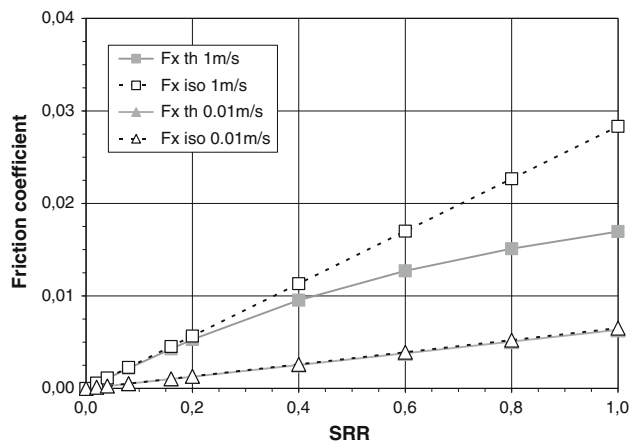


Fig. 2 Friction coefficient versus SRR predicted from isothermal and thermal EHL numerical models for two mean entrainment velocities, 1 and 0.01 m/s (glycerol, steel/steel smooth contact, $P_H = 1 \text{ GPa}$, $T = 323 \text{ K}$)

entrainment speed (0.01 m/s), isothermal and thermal friction coefficients are extremely close whereas at $U_e = 1$ m/s friction calculated with thermal effects significantly decreases compared to the isothermal case. This 40% friction drop is attributed to thermal heating [7] in the Hertzian zone of the contact area because any non-Newtonian behaviour is not allowed in the model (glycerol exhibits a high Newtonian limit). In addition, inlet shear heating remains moderate at 1 m/s, as indicated in Table 3. Finally, it is important to note that in all cases simulated here, friction coefficients are much lower than the ones obtained with classical paraffinic base oils.

2.2 Tribological Experiments

Traction measurements are performed with a ball-on-disc tribometer. The two specimens are driven by independent motors to produce the desired SRR with high precision and stability. They are made from bearing steel and they have been carefully polished to offer very smooth surfaces. The bottom of the ball dips into a reservoir containing 20 mL of glycerol, ensuring fully flooded conditions in the contact. The contact, the lubricant and the two shafts that support the specimens are thermally isolated from the outside and kept at constant temperature by an external thermal control system. This assembly was designed to limit heat transfer from or towards the contact zone, leading to experimental conditions as representative as possible of those considered in the numerical model. The experimental volume (i.e. the lubricant, the ball specimen and lower face of the disc) is also confined to prevent any air flow coming from the room environment. All parts that are likely to be in contact with the lubricant were previously cleaned up using a 3-solvent procedure to ensure the absence of any chemical contamination.

Traction forces and normal load are recorded by a multi-axis strain gauge sensor that combines a broad range of measurable forces, appropriate sensitivities over the different directions and a high stiffness that allows accurate traction measurements over a wide range of operating conditions [14, 15]. A platinum temperature probe, located approximately 2 mm underneath the ball specimen,

monitors the lubricant temperature in the test reservoir within ± 0.2 °C.

For all tests discussed in this article, the imposed temperature is 323 K, the SRR is 1.0 (disc running faster) and a normal load of 55 N is applied leading to a maximum contact pressure of approximately 1 GPa. Two different entrainment velocities are imposed in compliance with the general purpose of this study. $U_e = 1$ m/s leads theoretically to full separation and a TEHD lubrication regime whereas $U_e = 0.01$ m/s should correspond to the boundary regime characterized by λ values much lower than 1. λ is classically defined as follows:

$$\lambda = h_m / \sigma$$

where h_m is the minimum film thickness and σ is the composite r_{ms} roughness of the contacting surfaces.

Film thickness results reported in Fig. 1 indicate that $h_m = 180$ and 5 nm for $U_e = 1$ and 0.01 m/s, respectively. The actual roughness values are given in the following section; nevertheless considering a typical σ value of 10 nm, it becomes obvious that the low entrainment speed experiments can provide additional results that deal with the glycerol behaviour in the boundary regime.

Two long duration experiments were conducted, starting with $U_e = 1$ m/s for approximately 1 h, then applying $U_e = 0.01$ m/s during more than 20 h. Friction measurements and lubricant samplings were carried out at different times as indicated in Table 4. An important difference in the operating conditions between experiments 1 and 2 lies in the specimen roughness. In Experiment 1, the disc roughness represents the main contribution in σ , the composite r_{ms} value of the contacting surfaces, while the ball roughness could be considered as almost perfectly smooth. As for Experiment 2, the disc surface was kept identical but the ball polishing procedure was modified to produce a significant roughness increase compared to the finishing obtained in the first case. This change did not affect the friction coefficient measured at 1 m/s which remained remarkably constant and equal to 0.01; it is nearly 40% lower than values predicted by the TEHL model in Fig. 2. However, its influence is much more pronounced at

Table 4 Progress and operating conditions of Experiments 1 and 2 (glycerol, steel/steel contact, $P_H = 1$ GPa, $T = 323$ K)

Experiment 1 ($\sigma = 10$ nm)					Experiment 2 ($\sigma = 35$ nm)			
Time hh:mm	U_e m/s	Friction coeff.	Sample no.	Sampling time hh:mm	Time hh:mm	U_e m/s	Friction coeff.	Sample no.
00:00	1	0.0098	1	0:00	0:00	1	0.0105	5
1:05	1	0.0095	2	1:10	1:07	1	0.0093	
1:22	0.01	0.052			1:12	0.01	0.095 to 0.06	
6:48	0.01	0.023	3	5:25	6:18	0.01	0.048	
22:58	0.01	0.022	4	23:00	23:37	0.01	0.049	6

$U_e = 0.01$ m/s where higher friction values are observed for rougher surfaces (due to solid contact between metal asperities). This is in agreement with the predicted lubrication regimes: mixed-boundary regime ($\lambda = 0.5$, friction = 0.023) for Experiment 1 and boundary regime ($\lambda = 0.14$, friction = 0.048) for Experiment 2. Note that these friction values represent stabilized ones, obtained after 5 or 22 h of continuous rubbing and that larger friction coefficients were measured at the onset of the application of $U_e = 0.01$ m/s, meaning that some kind of running-in process occurred at this time.

Other differences exist in the progress of Experiments 1 and 2. Several glycerol samplings have been collected during Experiment 1 to detect the occurrence of any chemical change. The more severe conditions imposed during Experiment 2 offered the possibility of performing worn surface analysis and some glycerol sampling. The discussion on friction data, lubricant and surface analysis, regarding the applied operating conditions and the origin of tribo-mechanisms that could explain the obtained results, is presented in the next section.

2.3 Chemical and Surface Analyses

During experiments, four different samples of used glycerol were collected at different sampling times for Experiment 1 and two samples for Experiment 2 (see details in Table 4). The volume collected is about 1 mL at each time. Different chemical analyses of the liquid were performed including NMR, IR, GC/MS and eventually Karl Fischer for water detection. NMR analyses (BRUKER AVANCE 400) were performed at 30 °C with a QNP probe $^1\text{H}/^{13}\text{C}/^{19}\text{F}/^{31}\text{P}$ of 5 mm. Here ^1H NMR spectra (dilution in deuterated acetone) are only presented because the ^{13}C NMR spectra were very similar for all samplings. For pure glycerol (sample no. 1), two peaks are observed, one at 2.31 ppm from the 5 protons of the CH and CH_2 groups and a second one at 3.87 ppm corresponding to protons of the hydroxyl group (OH) in glycerol. In Table 5, the evolution of the peak at 3.87 ppm

Table 5 NMR and Karl Fischer analyses of the different samples collected (Table 4) during friction experiments

Sample	Integrated values of NMR peaks			Karl Fischer results (%)
	2.31 ppm	3.36 ppm	3.87 ppm	
1	5	–	3.046	0.36
2	5	0.021	2.976	–
3	5	0.031	2.971	–
4	5	0.077	2.953	1.24
5	–	–	–	0.62
6	–	–	–	3.25

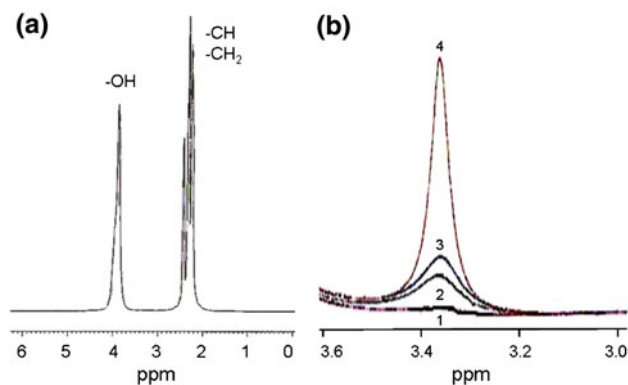
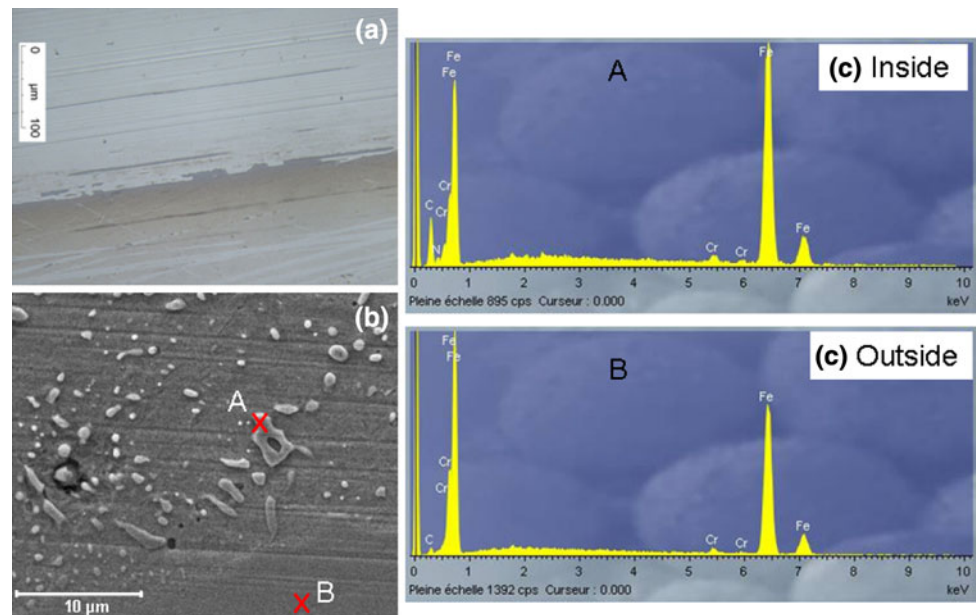


Fig. 3 a NMR spectrum of pure glycerol showing two characteristic peaks: one at 2.31 ppm from protons of the CH and CH_2 and one at 3.87 ppm corresponding to protons of the hydroxyl group (OH); b detail of the spectra of the four samples at 3.36 ppm showing the increase of a new peak characteristic of labile protons

(integrated values) is shown as a function of the test duration. The peak at 2.31 ppm does not show any change in the carbon skeleton of glycerol during the friction test. This result is confirmed by ^{13}C NMR spectra which show no change after the test (not shown here). In Fig. 3, the increase of a new peak in the ^1H NMR spectrum is observed at 3.36 ppm. This new line at 3.36 ppm is attributed to labile protons because a shift is observed when the spectrum is acquired at a higher temperature. This could be tentatively attributed to water molecules. Other ^1H NMR spectra (not shown) were recorded after dilution of glycerol in deuterated trichloromethane (CDCl_3): under these conditions, a new peak was observed at 8 ppm. This peak is possibly attributed to an aldehyde chemical group. Karl Fischer analyses are reported in Table 5. A slight increase is observed in the water content of glycerol from 0.36 to 1.24% for Experiment 1 and from 0.62 to 3.25% for Experiment 2. Then one can conclude that a tribochemical dissociation of glycerol is taking place during the duration of the friction test. Yet, it is very limited in quantity (a few per cent of molecules are eventually dissociated by the friction process).

SEM/EDX investigations on worn surfaces at the end of Experiment 2 are presented in Fig. 4. It is relatively amazing to see a corrosion pattern on the steel surface inside the wear scar where the experiment was stopped but not outside. The EDS spectra reveal that the white dots actually correspond to carbon, chromium (and Mn) carbide grains which are present in AISI 52100 steel material. This feature was already observed by some of the authors when using glycerol as a lubricant for steel under boundary lubrication conditions [4, 16]. This is another strong confirmation that the tribochemical reaction of glycerol liberates water as well as corrosive chemical compounds like acids and aldehydes, for example. These corrosive

Fig. 4 Wear track observed on the disc after friction experiment 2 with pure glycerol. **a** Optical image, **b** SEM image and **c** EDX spectrum: (A) inside and (B) outside



compounds are believed to leave the contact area after sliding. They come in contact with glycerol and can react to form glycerol acetate and water. Thus, corrosion of steel may not have the time to take place during the sliding. This is corroborated by the fact that no corrosion was observed in the case of static loaded contact where no sliding occurred. The thermal chemical dissociation of pure glycerol under moderate pressure and relatively high temperatures (400 MPa and $330\text{ }^{\circ}\text{C} < T < 430\text{ }^{\circ}\text{C}$) has been reported in the literature by Buehler [17] for example. The main products of the reaction have been analysed: water, ethanol, methanol, some aldehydes, acrolein, carbon monoxide and dioxide and hydrogen have been found. Moreover, water was a supercritical state in these experiments. Hence, it can be argued that such chemical dissociation routes are more likely to take place in the contact zone where high pressure and shear rates are encountered.

3 Discussion and Conclusions

Chemical analyses of glycerol lubricant after friction experiments show its partial tribochemical decomposition into water and other species. This result is reinforced by the difference observed between the friction coefficients measured and calculated at high velocity (1 m/s). The calculated friction is actually 70% higher than the measured one. This fact strongly suggests that glycerol is dissociated during its transit in the friction interface and that the water produced inside the contact zone reduces the traction force which is in agreement with recent work done by Klein et al. [18, 19]. Knowing the dimensions of the contact area (assuming a Hertzian diameter of $332\text{ }\mu\text{m}$), the sliding

speed and the film thickness (Fig. 2), one can easily evaluate the quantity of lubricant going through the contact during a given period of time. For example, in the case of 1 m/s mean entrainment speed, for a calculated film thickness of 300 nm, a lubricant volume flow rate through the contact of 0.36 mL per h was found. For 0.01 m/s and a film thickness of 14 nm, the volume flow rate becomes only 1.7×10^{-4} mL/h. During the test considered in this work (1 h at 1 m/s and 20 h at 0.01 m/s), the total volume of glycerol that passed through the contact is about 0.4 mL compared to the 20 mL contained in the reservoir and dissociation comes mainly from the first step in the high speed regime (1 m/s). This indicates that the increase in the water content of 1% in the whole glycerol quantity (which corresponds approximately to 0.2 mL) does not reflect the water content which is effectively produced in the contact zone. A rough estimation of the glycerol/water conversion produced in the 300 nm thick EHL film is at least 40%. However, the homogeneity of the water/glycerol mixture is certainly not constant throughout the whole experimental volume.

At this stage, it is interesting to consider the rheological properties of water-in-glycerol mixtures and their effect on film thickness and friction. From the literature [20], the viscosity of glycerol is about 140 mPa s but it drastically decreases to about 4 mPa s when 40% of water is added at an operating temperature of $50\text{ }^{\circ}\text{C}$. Such an effect could be implemented in the TEHL numerical model to compare experimental and predicted film thickness and friction in the presence of water. However, taking into account in the same time pressure, temperature and water concentration to get a proper estimate of water–glycerol mixture viscosity within the operating conditions investigated at this study

should be thoroughly conducted. As previously mentioned, we used data from Cook et al. [8] for pure glycerol. Similarly we used references [21, 22] and [23] for pure water and glycerol–water mixtures, respectively. The parameters of the Cheng equation [11] were thus derived for each water-in-glycerol mass concentration to define the viscosity–pressure–temperature relationship. Thus, numerical TEHL simulations were run assuming a Newtonian behaviour for water-in-glycerol mass concentrations varying from 0 to 40% and the results are reported in Figs. 5 and 6.

Under pure rolling conditions (Table 3 shows that SRR had a weak influence on h_c and h_m for pure glycerol), one can note that both central (Fig. 5a) and minimum film thicknesses (Fig. 5b) are reduced by an order of magnitude when the water mass concentration increases from 0 to 40%. However, because both water conversions are likely to occur in the central part of the contact and film thickness mainly results from hydrodynamic effects occurring in the contact inlet, one can consider that a limited thickness

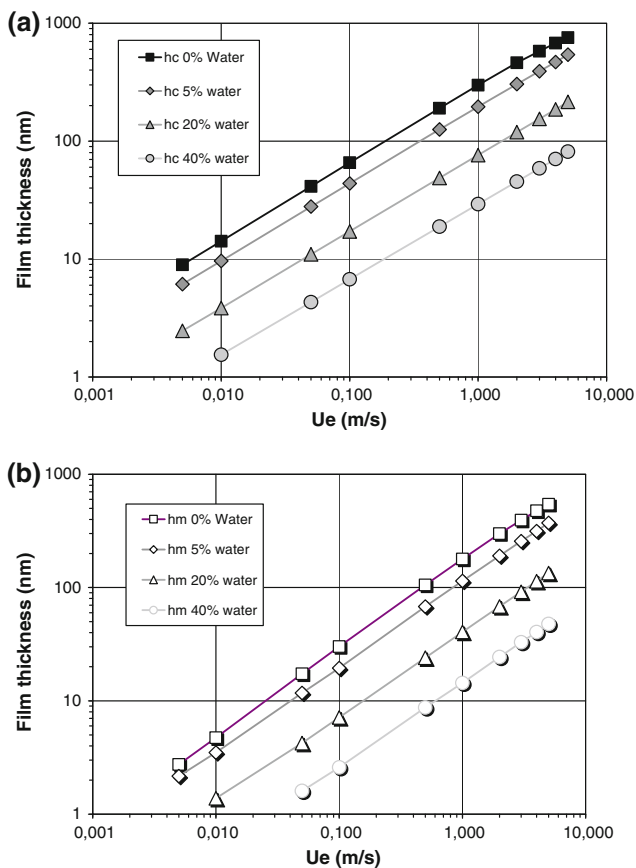


Fig. 5 Central (h_c , a) and minimum (h_m , b) film thickness versus mean entrainment velocity (U_e) predicted for several water-in-glycerol mass fractions (thermal EHL model, steel/steel smooth contact, pure rolling, $P_H = 1$ GPa, $T = 323$ K)

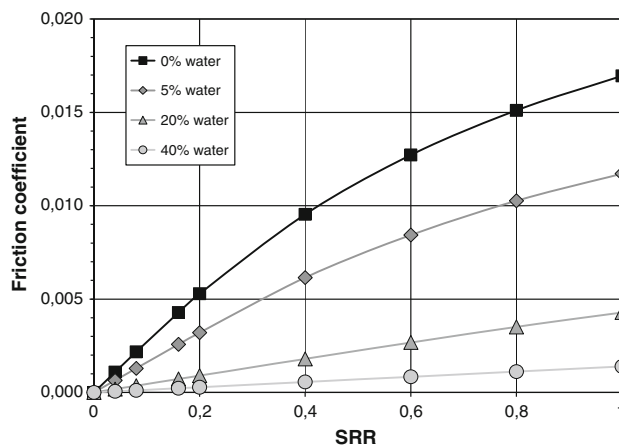


Fig. 6 Friction coefficient versus SRR predicted for several water-in-glycerol mass fractions (thermal EHL model, 1 m/s, steel/steel smooth contact, $P_H = 1$ GPa, $T = 323$ K)

reduction should happen. On the other hand, the situation is totally changed when considering friction because the latter is mainly generated in the central part of the contact where water is generated. Due to the design of the tribometer and the relatively high viscosity of the pure glycerol, most of the water produced within the contact is likely to remain close to the sphere location. Thus, larger concentrations of water can be present in the high pressure contact area and can strongly influence friction. Numerical results obtained under rolling-sliding conditions ($SRR = 1$, as during experiments) show in Fig. 6 that friction is reduced by 30% when the water content reaches 5% and by 75% when the water percentage reaches 20%. This simulation is not in good agreement with the glycerol/water conversion of 40% for a reduction of 70% of friction. However, the simulation does not consider that the fluid entering the EHL contact is practically pure glycerol and not a glycerol/water mixture. More study is necessary to simulate this particular case.

Acknowledgments The authors thank Nathalie Bouscharain and Nicolas Devaux (LaMCoS, INSA-Lyon) for their contribution to the experimental part of this study.

References

1. Kano, M., Yasuda, Y., Okamoto, Y., Mabuchi, Y., Hamada, T., Ueno, T., Ye, J., Konishi, S., Takeshima, S., Martin, J.M., De Barros Bouchet, M.I., Le Mogne, T.: Ultralow friction of DLC in presence of glycerol mono-oleate (GMO). *Tribol. Lett.* **18**(2), 245–251 (2005)
2. De Barros Bouchet, M.I., Matta, C., Le Mogne, T., Martin, J.M., Sagawa, T., Okuda, S., Kano, M.: Improved mixed and boundary lubrication with glycerol-diamond technology. *Tribology* **1**(1), 28–32 (2007)
3. Joly-Pottuz, L., Matta, C., De Barros Bouchet, M.I., Vacher, B., Martin, J.M., Sagawa, T.: Superlow friction of ta-C lubricated by

- glycerol: an electron energy loss spectroscopy study. *J. Appl. Phys.* **102**, 064912 (2007)
4. Matta, C., Joly-Pottuz, L., De Barros Bouchet, M.I., Martin, J.M., Kano, M., Zhang, Q., Goddard III, W.A.: Superlubricity and tribochemistry of polyhydric alcohols. *Phys. Rev. B* **78**, 085436 (2008)
 5. Bair, S.: High-pressure rheology for quantitative elastohydrodynamics. Elsevier BV, Amsterdam (2007)
 6. Vergne, P.: Super low traction under EHD and mixed lubrication regimes. In: Erdemir, A., Martin, J.M. (eds.) Superlubricity, pp. 429–445. Elsevier BV, Amsterdam (2007)
 7. Habchi, W., Eyheramendy, D., Vergne, P., Bair, S., Morales-Espejel, G.E.: Thermal elastohydrodynamic lubrication of point contacts using a Newtonian/generalized Newtonian lubricant. *Tribol. Lett.* **30**(1), 41–52 (2008)
 8. Cook, R.L., King, H.E., Herbst, C.A., Herschback, D.R.: Pressure and temperature dependent viscosity of two glass forming liquids: glycerol and dibutyl phthalate. *J. Chem. Phys.* **100**(7), 5178–5189 (1994)
 9. Bridgman, P.W.: The physics of high pressure. Dover, New York (1970)
 10. Lide, D.R.: CRC handbook of chemistry and physics, 85th edition, CRC press, Boca Raton (2004–2005)
 11. Cheng, H.S., Sternlicht, B.: A numerical solution for the pressure, temperature and film thickness between two infinitely long, lubricated rolling and sliding cylinders under heavy loads. *ASME J. Basic Eng.* **87**, 695–707 (1965)
 12. Hirschfelder, J.O., Curtiss, C.F., Bird, R.B.: Molecular theory of gases and liquids. Wiley, New York (1954)
 13. Hogenboom, D.L., Webb, W., Dixon, J.D.: Viscosity of several liquid hydrocarbons as a function of temperature, pressure and free volume. *J. Chem. Phys.* **46**(7), 2586–2598 (1967)
 14. Bair, S., Vergne, P., Query, M.: A unified shear-thinning treatment of both film thickness and traction in EHD. *Tribol. Lett.* **18**(2), 145–152 (2005)
 15. Yagi, K., Vergne, P.: Abnormal film shapes in sliding EHD contacts lubricated by fatty alcohols. *Proc. I Mech. E. J* **221**(3), 287–300 (2007)
 16. Joly-Pottuz, L., Martin, J.M., De Barros Bouchet, M.I., Belin, M.: Anomalous low friction under boundary lubrication of steel surfaces by polyols. *Tribol. Lett.* **34**, 21–29 (2009)
 17. Bühler, W., Dinjus, E., Ederer, H.J., Kruse, A., Mas, C.: Ionic reactions and pyrolysis of glycerol as competing reaction pathways in near- and supercritical water. *J. Supercrit. Fluids* **22**, 37–53 (2002)
 18. Briscoe, W.H., Titmuss, S., Tiberg, F., Thomas, R.K., McGilivray, D.J., Jacob, K.: Boundary lubrication under water. *Nat. Lett.* **444**, 191–194 (2006)
 19. Raviv, U., Klein, J.: Fluidity of bound hydration layers. *Science* **297**, 1540–1543 (2002)
 20. Dorsey, N.E.: Properties of ordinary water-substance, p. 184, Hafner Publishing Co., New York (1940)
 21. Tanishita, I., Nagashima, A., Murai, Y.: Correlation of viscosity, thermal conductivity and Prandtl number for water and steam as a function of temperature and pressure. *Bull. JSME* **14**(77), 1187–1198 (1971)
 22. Bett, K.E., Cappi, J.B.: Effect of pressure on the viscosity of water. *Nature* **207**(4997), 620–621 (1965)
 23. Shankar, P.N., Kumar, M.: Experimental determination of the kinematic viscosity of glycerol-water mixtures. *Proc. R. Soc. Lond. A* **444**, 573–581 (1994)